

## **Well-Ordered Mesoporous Silica Prepared by Cationic Fluorinated Surfactant Templating**

Stephen E. Rankin<sup>\*§</sup>, Bing Tan<sup>§</sup>, Hans-Joachim Lehmler<sup>†</sup>, Kimberly P. Hindman<sup>§</sup> and Barbara L. Knutson<sup>§</sup>

<sup>§</sup> Chemical and Materials Engineering Department, University of Kentucky,  
Lexington, KY 40506-0046, U.S.A.

<sup>†</sup> Department of Occupational and Environmental Health, University of Iowa, College of Public  
Health, Iowa City, IA 52242-5000 U.S.A.

\* To whom correspondence should be addressed. Phone: +1-859-257-9799. E-mail:  
srankin@engr.uky.edu.

### **Abstract**

We describe the synthesis and characterization of ordered mesoporous silica using the template 1H,1H,2H,2H-perfluorooctylpyridinium chloride. This surfactant forms several lyotropic mesophases at room temperature, including hexagonal close packed cylinders, an isotropic liquid crystal, and a lamellar phase. Using this surfactant, mesoporous silica is synthesized by room temperature precipitation and surfactant extraction. Both the surfactant and product material are thoroughly characterized. From nitrogen adsorption, the product has a specific surface area of 982 m<sup>2</sup>/g and a pore diameter of 2.6 nm. X-ray diffraction and transmission electron microscopy confirm 2-dimensional close-packed hexagonal long-range ordering. This is the first example of cationic fluorinated surfactant templating of an ordered porous ceramic material.

Keywords: Surfactant templating, silica, mesoporous, fluorinated

## Introduction

Since their discovery[1], researchers have tried to control the size, structure and orientation of the pores in surfactant-templated silica[2,3]. These materials are formed by co-assembly of surfactants and silica precursors, followed by silica network formation and surfactant removal by calcination or extraction. All major classes of hydrocarbon surfactants (cationic, nonionic and anionic)[4] including single- and double-[5] tailed surfactants have been used as templates. It has been shown that the pore size decreases as the length of the alkyl chain decreases for alkyltrimethylammonium halide templates, but that the ability of these surfactants to form well-ordered assemblies with silica diminishes for chains shorter than decyl. Octyl chains give uniform pores without long-range order, unless double-tailed surfactants are added to promote micelle ordering[6]. This limitation is significant, because it leaves unspanned the gap in pore size between zeolites (maximum pore size ~1.4 nm for aluminophosphates[7]) and ordered surfactant-templated silica (pore sizes > 2.7 nm unless double-tailed surfactants are used[6]).

However, fluorinated surfactants are a qualitatively different class of surfactants that have not yet been explored extensively. There has to date been one report of using a fluorinated surfactant in combination with a nonionic block copolymer as a template for mesoporous silica[8], but the pore size does not seem to be related to the fluorosurfactant used. In that report, the precise role of the fluorinated surfactant in the pore templating process is not entirely clear. In fact, Han et al. suggest that "...fluorocarbon surfactants are not suitable as templates for the preparation of well-ordered materials." [9] However, fluorinated surfactants form aggregates more easily and with lower curvature than their hydrocarbon analogues[10,11]. This suggests that they may be suitable as porogens, if the right surfactant and synthesis conditions were chosen. The strong carbon-fluorine bond also causes them to have strikingly different molecular

interactions than hydrocarbon surfactants[10]. While this paper was under review, Blin et al. published the first example of mesoporous silica synthesized with only a fluorinated surfactant template, in their case a nonionic surfactant.[12] In this brief article, we will show that cationic fluorinated surfactants also can be used as templates for ordered porous ceramics and that their ease of assembly allows small-pore ordered structures to be formed from a single-tailed surfactant.

### **Experimental Methods**

The surfactant, 1H,1H,2H,2H-perfluorooctylpyridinium chloride (FSPCl-1) was synthesized as described previously, by alkylation of anhydrous pyridine with 1H,1H,2H,2H-perfluorooctyl iodide.[13] The resulting pyridinium iodide was carefully washed with anhydrous diethyl ether and recrystallized from acetone. The corresponding chloride was obtained by ion exchange chromatography on Amberlite IRA-410 and used without further purification. Melting points were determined using a Thermal Analysis 2920 Differential Scanning Instrument. Thermograms were recorded using a heating rate of 20°/minute from 20 to 230°C and the onset temperatures of the main transitions were determined.[14] Mass spectra were recorded at the University of Kentucky Mass Spectrometry Facility using a Kratos Kompact SEQ or Bruker Autoflex time-of-flight mass Spectrometer equipped with MALDI. The formula weight of the pyridinium cation of both the iodide and chloride surfactants was 426 g/mol.

Materials were prepared by first adding 0.750 g aqueous ammonium hydroxide (~28 wt%) and 0.400 g FSPCl-1 to 13.9 g of deionized ultrafiltered water. After mixing for one hour, 1.08 g of tetraethoxysilane (TEOS) was slowly added with continuous stirring. Within two minutes after the addition of TEOS to the surfactant solution, a white powder precipitated. The solution was aged at room temperature for 24 hr and then filtered. The as-synthesized material was dried

in air for 48 hr. The surfactant was extracted from the dried material by twice stirring with a mixture of 150 ml ethanol (95 wt% with water) and 5 ml aqueous HCl (~36 wt%) for 24 hr, followed by filtration. The shorthand notation for this sample will be UK-1.

Samples for FTIR analysis were ground finely, mixed with KBr at a concentration of 1 wt% of the sample, and pressed into translucent pellets. Spectra were collected with a ThermoNicolet Nexus 470 spectrometer. Nitrogen sorption isotherms of the samples after surfactant extraction and drying were collected with a Micromeritics Tristar 3000 automated adsorption instrument. The samples were outgassed for 4 hours at 150 °C. X-ray powder diffraction (XRD) patterns were recorded with a Siemens 5000 diffractometer using 1.54098 nm CuK $\alpha$  radiation. Powders were mixed with a small amount of acetone and pressed into a holder. For transmission electron microscopy (TEM), samples were ground, suspended in acetone and deposited on lacey carbon TEM grids for analysis with a JEOL 2010F instrument.

## Results and Discussion

The surfactants were thoroughly characterized for purity and composition. The results of the DSC and NMR investigations of the surfactants are as follows:

### *1H,1H,2H,2H-perfluorooctyl pyridinium iodide:*

m.p. = 110, 130, 170 and 186°C. <sup>1</sup>H-NMR (DMSO, 400 MHz)  $\delta$  3.14-3.32 (m, -CH<sub>2</sub>CF<sub>2</sub>-, 2H), 5.02 (t, -CH<sub>2</sub>CH<sub>2</sub>CF<sub>2</sub>,  $J$  = 7.2 Hz), 8.23 (“t”,  $J$  ~ 7.0 Hz, 2H), 8.68 (t,  $J$  = 8.0 Hz, t,  $J$  = 1.2 Hz, 1H), 9.23 (“d”,  $J$  ~ 5.2 Hz, 2H) ppm. <sup>13</sup>C-NMR (DMSO, 100 MHz)  $\delta$  30.55 (t, -CH<sub>2</sub>CF<sub>2</sub>-,  $J_{CF}$  = 20 Hz), 52.83(t, -CH<sub>2</sub>CH<sub>2</sub>CF<sub>2</sub>), 128.07, 145.52, 146.34 ppm. <sup>19</sup>F-NMR (D<sub>3</sub>COD, 376 MHz)  $\delta$  -81.63 (-CF<sub>3</sub>), -113.67, -122.10, -123.12, -123.58, 126.57 ppm.

### *1H,1H,2H,2H-perfluorooctyl pyridinium chloride (FSPCl-1)*

m.p. = 178°C.  $^1\text{H-NMR}$  (DMSO, 400 MHz)  $\delta$  3.14-3.32 (m,  $-\text{CH}_2\text{CF}_2-$ , 2H), 5.02 (t,  $-\text{CH}_2\text{CH}_2\text{CF}_2$ ,  $J = 7.2$  Hz), 8.20 (“t”,  $J \sim 7.0$  Hz, 2H), 8.69 (t,  $J = 8.0$  Hz, t,  $J = 1.2$  Hz, 1H), 9.18 (“d”,  $J \sim 5.2$  Hz, 2H) ppm.  $^{13}\text{C-NMR}$  (DMSO, 100 MHz)  $\delta$  30.55 (t,  $-\text{CH}_2\text{CF}_2-$ ,  $J_{\text{CF}} = 20$  Hz), 52.83(t,  $-\text{CH}_2\text{CH}_2\text{CF}_2$ ), 128.07, 145.52, 146.34 ppm.  $^{19}\text{F-NMR}$  ( $\text{D}_3\text{COD}$ , 376 MHz)  $\delta$  -81.65 ( $-\text{CF}_3$ ), -113.73, -122.13, -123.14, -123.64, 126.60 ppm.

Before attempting to synthesize materials, we used polarization contrast optical microscopy to rapidly scan the phase behavior of FSPCl-1. The phase diagram of 1H,1H,2H,2H-perfluorodecylpyridinium chloride was recently reported, and hexagonal close packed cylindrical phases were found to be less favorable near room temperature than “intermediate” phases such as rectangular and mesh phases at room temperature<sup>[15]</sup>. Therefore, we could not be sure *a priori* whether our surfactant would be able to form conventional pore structures such as hexagonal close packed cylinders. Figure 1a shows the results of a flooding experiment, in which a solid crystal of surfactant was surrounded with deionized ultrafiltered water. The solid material was initially near the top center of the figure, so the concentration decreases moving away from the point. The micrograph was collected very shortly after the water was introduced. Moving outward, transitions are seen from a lamellar structure (near the center) to an isotropic liquid crystal phase (the black band) to a hexagonal close packed phase, to an isotropic micellar phase.

Samples were also prepared of well defined composition and allowed to equilibrate at room temperature ( $22 \pm 1$  °C) for 72 hours. Figure 1b shows that a 50 wt% solution in water has a hexagonal close packed (HCP) structure, as indicated by the fanlike texture. The 60 wt% solution also has a HCP structure (not shown). Figure 1c shows that a 70 wt% solution of FSPCl-1 in water has a lamellar structure, indicated by the “streaky” appearance of the birefringence texture. This rapid screening study of the phase behavior of the surfactant suggests

that it may be possible to prepare a material with HCP, isotropic liquid crystal, or lamellar structure.

With the confirmation that our surfactant is able to form ordered mesophases at room temperature, we discuss the synthesis. Infrared spectroscopy (Figure 2) confirms that we incorporate FSPC1-1 into the silica particles, and that our extraction procedure completely removes the surfactant. The solid surfactant spectrum (Fig. 2a) shows several bands in the range ( $1400\text{ cm}^{-1}$  to  $700\text{ cm}^{-1}$ ) associated with fluorinated alkyl groups.[16,17] Of these bands, the most prominent ones have been assigned to asymmetric  $\text{CF}_2$  stretching ( $1247\text{ cm}^{-1}$ ), CCC deformation ( $1207\text{ cm}^{-1}$ ), and symmetric  $\text{CF}_2$  stretching ( $1147\text{ cm}^{-1}$ ).[16,17] In the as-synthesized material (Fig. 2b) all of these bands may be present, but the  $1147\text{ cm}^{-1}$  band is most clearly defined (indicated with an arrow). In the extracted product (Fig. 2c), the  $1147\text{ cm}^{-1}$  band cannot be observed, but there still is a shoulder at about  $1200\text{ cm}^{-1}$ . This shoulder is typical of high-surface area silica[18,19] and, like the more prominent band at  $1093\text{ cm}^{-1}$ , is assigned to asymmetric Si-O-Si stretching.[20] The spectrum of fumed silica (>99%, Aldrich) shown in Fig. 2d has the same features as the extracted material, and confirms the assignment of the shoulder at  $1200\text{ cm}^{-1}$  to silica. A clearer indication of the presence of the surfactant in the as-synthesized product (Fig. 2b) is the narrow band at  $1495\text{ cm}^{-1}$  that does not coincide with any other bands. This band has not been assigned to fluorocarbons[17] and is more likely to be associated with pyridinium motion. After 2 extraction steps, this band is completely absent (Fig. 2c).

The nitrogen adsorption isotherm after surfactant extraction is shown in Figure 3. This type IV isotherm has an inflection at  $p/p_0 = 0.116$ , suggesting that capillary condensation in uniform pores is occurring. To learn more about the pore structure, we prepared and analyzed an  $\alpha_s$ -plot

according to the procedure of Sayari et al.[21]. Data for the macroporous reference material, LiChrospher Si-1000, are taken from Jaroniec et al.[22].

Analysis of the  $\alpha_s$  plot determines features of the structure of these materials without reference to a particular adsorption model (other than the BET method used to determine the surface area of the reference material[22], 22.1 m<sup>2</sup>/g). We observe the same features as have been observed for other mesoporous silicates[21]. A line fit through the data at low  $\alpha_s$  passes through the origin, indicating that the product does not contain micropores. The slope of this line gives the total specific surface area of the sample,  $S_t$ . After capillary condensation ends, adsorption continues outside of the mesopores, and the slope of a second line at high  $\alpha_s$  gives the external specific surface area,  $S_{ext}$ . These results, and the BET surface area[23], are reported in Table 1. Extrapolating the external adsorption (high- $\alpha_s$ ) line to  $\alpha_s = 0$  gives the primary pore volume ( $V_p$ ).

Availability of well-defined porous silica has recently led to improved methods for determining the size of cylindrical silica pores by nitrogen adsorption. A modified Kelvin equation approach (the KJS method) has been shown to give accurate estimates of pore size for MCM-41 materials[24]. In the inset of Figure 3, we show the pore size distribution calculated using the KJS method. The peak pore diameter,  $d_{KJS}$ , is given in Table 1. Consistent results are found using non-local density functional theory values[25], based on the position of the inflection in the isotherm ( $d_{NLDFT}$ ), or from a simple geometric calculation based on the assumption of cylindrical pores.

Values calculated by the KJS method, NLDFT, and geometric methods are all consistent with a pore diameter of 2.6 nm. This disagrees with the prediction of the often-used BJH method[26], 1.9 nm. The BJH method is known to underpredict pore diameters near the

micropore-mesopore boundary[27] so other estimates can be considered to be more reliable. A similar pore diameter was recently reported when a large amount of the cosurfactant butylamine was added to an MCM-41 synthesis solution, but the long-range ordering of that material was limited (as indicated by only two diffraction peaks)[28].

To demonstrate long-range order in sample UK-1, XRD results are presented in Figure 4 for the as-prepared and extracted samples. The as-prepared sample (dashed line) shows poorly resolved peaks, probably because of poor contrast between silicon and the fluorocarbon surfactant. The most clearly resolved peak has a d-spacing of 2.8 nm. The extracted sample (solid line) clearly shows evidence for three diffraction peaks which are indexed according to a 2D hexagonal close packed (HCP) structure. Contrasting this, MCM-41 prepared using octyltrimethylammonium bromide has a uniform pore size, but no evidence from higher-order diffraction peaks of well-defined order [29].

Extraction of the surfactant from UK-1 does not change the d-spacing of the (100) peak significantly (it is 2.83 nm). The unit cell size for the 2D HCP structure is  $3.28 \pm 0.01$  nm. Based on the pore size estimated above, this gives an approximate wall thickness of 0.7 nm. The diffraction peaks are relatively broad, and from the Scherrer equation, we estimate a scattering domain size of approximately 13 nm.

TEM confirms the presence of cylindrical pores with 2D hexagonal symmetry. Figure 5 shows two representative images of UK-1 after surfactant extraction. Figure 5a shows a direct image of the 2D HCP structure. A Fourier transform of this region (inset) shows six spots characteristic of a 2D HCP structure. Figure 5b shows a region with layers of light and dark stripes. The Fourier transform of this region (inset) shows two spots characteristic of a lamellar structure. However, the image is also consistent with a 2D HCP cylindrical structure viewed

from the edge of the cylinders. The spacing between layers is consistent with the 2D HCP (100) d-spacing measured by XRD. There is no indication from XRD or from TEM sampling that lamellar regions are actually present in our sample. Because there is no orientation preference in these particles, other parts of the image appear to be disordered, but that could be due to superposition of ordered regions with different orientations. The observation of small oriented domains in the TEM images is consistent with the broad XRD peaks observed in Figure 4.

## **Conclusions**

Using a partially fluorinated octylpyridinium chloride surfactant, we synthesized silica particles with 2.6 nm, 2D hexagonal close packed cylindrical pores. The pore size was confirmed by several theoretical interpretations of the nitrogen adsorption data. The long-range 2D hexagonal ordering was confirmed by XRD and TEM. This is the first time that a cationic fluorinated surfactant alone has been used as the template for ordered mesoporous silica. This also is the first time that a single-tailed surfactant has been used to generate a porous material with long-range order from a cationic octyl surfactant. This finding suggests that fluorinated surfactants may have potential to further reduce the available pore sizes in surfactant templated porous ceramic materials. We are currently investigating in detail the effects of fluorinated surfactant architecture and synthesis conditions on the pore structure of these materials.

## **Acknowledgments**

We thank Prof. Elizabeth Dickey and Ms. Colleen Frazer of Pennsylvania State University for helpful discussions of the characterization. We thank Dr. Alan Dozier of the University of Kentucky Materials Characterization Facility for his help with the TEM. We thank Prof. Kimberly Anderson of the University of Kentucky and her group for helping with the use of the optical microscope. This material is based upon work supported by the National Science

Foundation under Grant No. DMR-0210517. BT was supported by a Kentucky Research Challenge Trust Fund graduate fellowship.

## REFERENCES

- [1] C.T. Kresge et al., *Nature* 359 (1992) 710.
- [2] U. Ciesla, F. Schüth, *Microporous and Mesoporous Mater.* 27 (1999) 131.
- [3] J.Y. Ying et al., *Angew. Chem. Int. Ed.* 38 (1999) 56.
- [4] Q.S. Huo et al., *Nature* 368 (1994) 317.
- [5] Q. Huo et al., *Chem. Mater.* 8 (1996) 1147.
- [6] R. Ryoo et al., *J. Am. Chem. Soc.* 123 (2001) 1650.
- [7] M.E. Davis, *Chem. Eur. J.* 3 (1997) 1745.
- [8] Y. Han et al., *Angew. Chem. Int. Ed.* 42 (2003) 3633.
- [9] *ibid*, p. 3633
- [10] M.P. Krafft, J.G. Riess, *Biochim.* 80 (1998) 489.
- [11] M. Monduzzi, *Current Opinion in Colloid & Interface Science* 3 (1998) 467.
- [12] J.L. Blin et al., *Langmuir* 20 (2004) 491.
- [13] T. Asakawa et al., *Langmuir* 11 (1995) 478.
- [14] H.J. Lehmler et al., *Journal of Fluorine Chemistry* 107 (2001) 141.
- [15] K. Wang et al., *Langmuir* 16 (2000) 1042.
- [16] S.L. Hsu et al., *Macromolecules* 23 (1990) 4565.
- [17] Y. Ren et al., *J. Chem. Phys.* 113 (2000) 1162.
- [18] S.M. Holmes et al., *J. Chem. Soc., Faraday Trans.* 94 (1998) 2025.
- [19] D.C. Calabro et al., *Microporous Materials* 7 (1996) 243.
- [20] E.I. Kamitsos et al., *Phys. Rev. B* 48 (1993) 12499.
- [21] A. Sayari et al., *Chemistry of Materials* 9 (1997) 2499.
- [22] M. Jaroniec et al., *Langmuir* 15 (1999) 5410.
- [23] S. Brunauer et al., *J. Am. Chem. Soc.* 60 (1938) 309.
- [24] M. Kruk et al., *Langmuir* 13 (1997) 6267.
- [25] P.I. Ravikovitch et al., *Langmuir* 11 (1995) 4765.
- [26] E.P. Barrett et al., *J. Am. Chem. Soc.* 73 (1951) 373.
- [27] A.V. Neimark et al., *Journal of Colloid and Interface Science* 207 (1998) 159.
- [28] F. Kleitz et al., *Langmuir* 18 (2002) 4963.
- [29] J. Choma et al., *Coll. Surf. A: Phys. Eng. Aspects* 203 (2002) 97.

**Table 1.** Nitrogen adsorption analysis results for sample UK-1

$S_t$ (m <sup>2</sup> /g)	$S_{ext}$ (m <sup>2</sup> /g)	$S_{BET}^a$ (m <sup>2</sup> /g)	$V_p$ (cm <sup>3</sup> /g)	$d_{KJS}$ (nm)	$d_{NLDFT}$ (nm)	$4V_p/(S_t-S_{ex})$ (nm)	$d_{BJH}$ (nm)
982.	39.4	1134	0.608	2.57	2.60	2.58	1.90

<sup>a</sup> Calculated using data in range of p/p<sub>0</sub> from 0.04 to 0.1.

**Figure captions**

**Figure 1.** Polarization contrast micrographs of FSPCl-1 solution in water at room temperature.

(a) Low-magnification view immediately after flooding a single particle of solid surfactant with deionized water, (b) 200x magnification view of equilibrated sample of 50 wt% surfactant, and (c) 200x view of equilibrated sample of 70 wt% surfactant.

**Figure 2.** FTIR spectra of KBr pellets pressed with 1 wt% of (a) the pure surfactant, FSPCl-1, (b) sample UK-1 as synthesized, (c) sample UK-1 after extraction, and (d) fumed silica. The arrows indicate surfactant bands in the as-synthesized product that are absent after extraction.

**Figure 3.** Adsorption isotherm for sample UK-1. Filled circles are adsorption points and open circles are desorption points. The inset shows the pore size distribution of sample UK-1 after extraction calculated by the KJS method [24].

**Figure 4.** XRD results for sample UK-1 as-prepared (lower) or after extraction (upper).

**Figure 5.** Representative transmission electron micrographs of UK-1 after surfactant extraction. The views illustrate (a) a 2D HCP region and (b) a striped region consistent with the 2D HCP structure viewed from the edge of the cylindrical pores. The insets show Fourier transforms of the images.

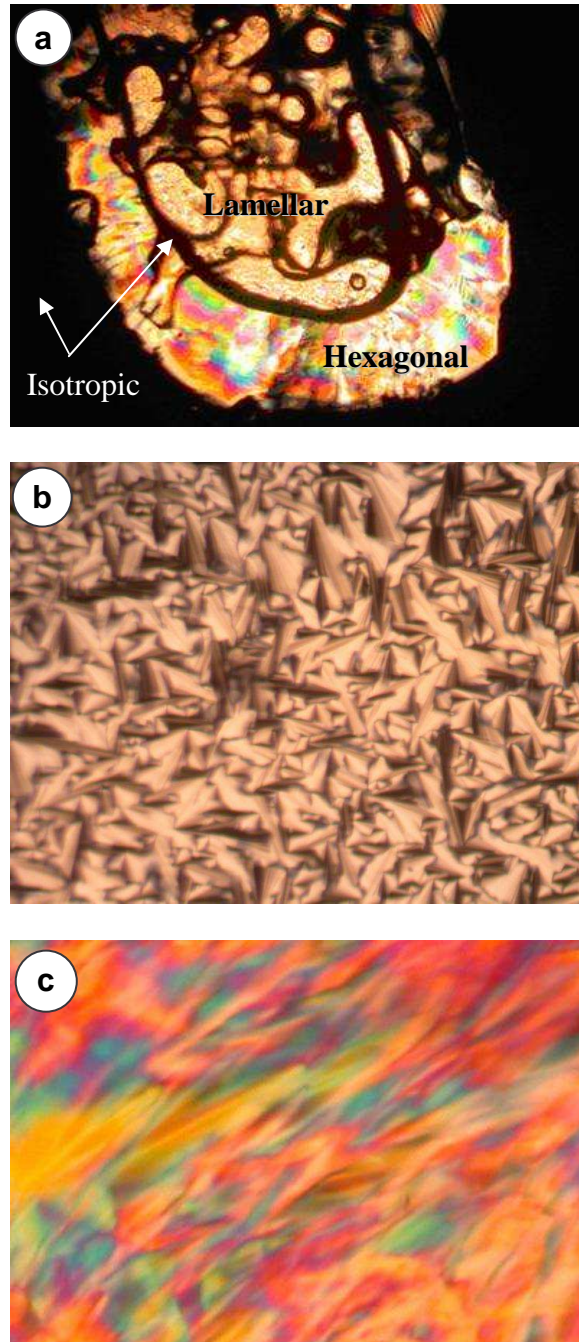


Figure 1

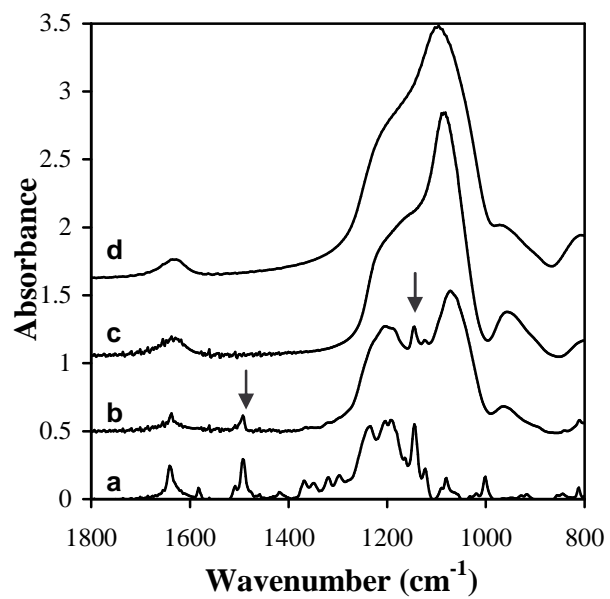


Figure 2

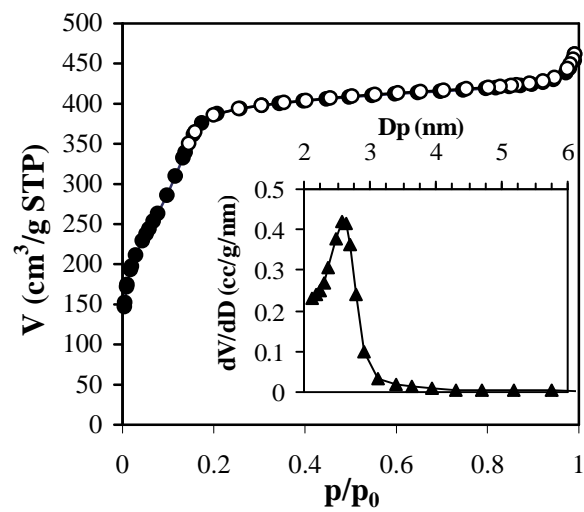


Figure 3

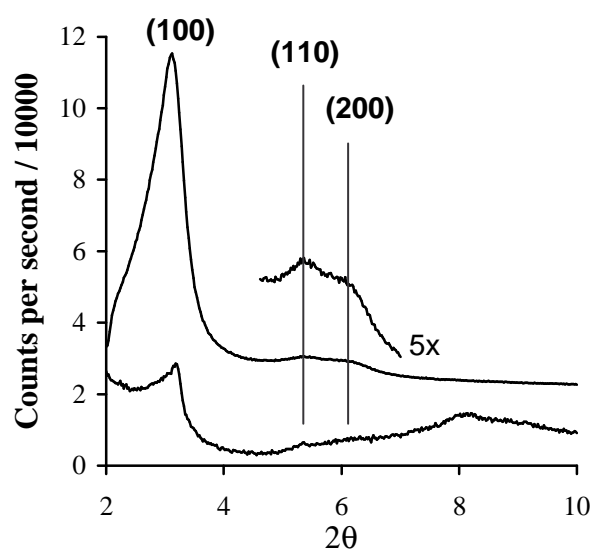


Figure 4

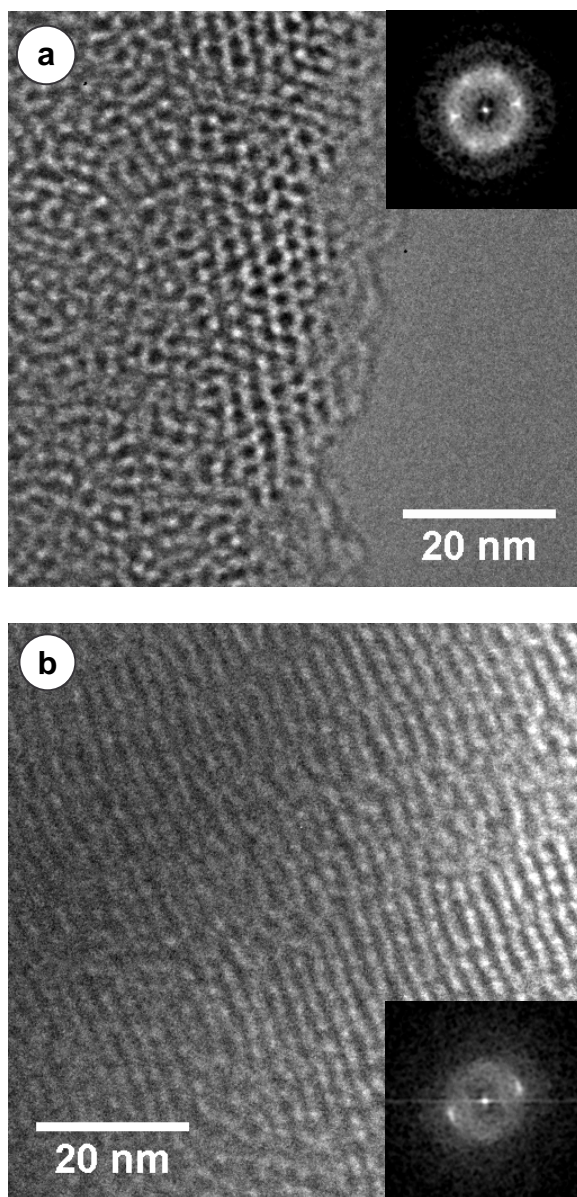


Figure 5